

## Thioridazine inhibits autophagy and sensitizes glioblastoma cells to temozolomide

Tor-Christian Aase Johannessen<sup>1,5,14</sup>, Md Abdul Mahdi Hasan-Olive<sup>1,14</sup>, Huaiyang Zhu<sup>1,7,14</sup>, Oxana Denisova<sup>11</sup>, Amra Grudic<sup>1,6</sup>, Md Latif<sup>d</sup>, Halala Saed<sup>1</sup>, Jobin K. Varughese<sup>1</sup>, Gro Vatne Røsland<sup>12</sup>, Ning Yang<sup>1,8,9</sup>, Terje Sundstrøm<sup>1,6</sup>, Anne Nordal<sup>4</sup>, Karl Johan Tronstad<sup>12</sup>, Jian Wang<sup>1,8,9</sup>, Morten Lund-Johansen<sup>6,10</sup>, Anne Simonsen<sup>13</sup>, Bassam Janji<sup>3</sup>, Jukka Westermarck<sup>11</sup>, Rolf Bjerkvig<sup>1,2,15</sup> and Lars Prestegarden<sup>1,4,10,15</sup>.

<sup>1</sup>Kristian Gerhard Jebsen Brain Tumor Research Centre, Department of Biomedicine, University of Bergen, Jonas Lies Vei 91, 5009 Bergen, Norway;

<sup>2</sup>NorLux Neuro-Oncology Laboratory, Department of Oncology, Luxembourg Institute of Health, 84 Val Fleuri, 1526 Luxembourg.

<sup>3</sup>Laboratory of Experimental Hemato-Oncology, Department of Oncology, Luxembourg Institute of Health (LIH), Luxembourg City, Luxembourg.

<sup>4</sup>Department of Dermatology, Haukeland University Hospital, Haukelandsveien 22, 5021 Bergen, Norway

<sup>5</sup>Department of Oncology, Haukeland University Hospital, Haukelandsveien 22, 5021 Bergen, Norway

<sup>6</sup>Department of Neurosurgery, Haukeland University Hospital, Haukelandsveien 22, 5021 Bergen, Norway

<sup>7</sup>Department of Oncology, Shandong Chest Hospital, 250013, Jinan, China

<sup>8</sup>Department of Neurosurgery, Qilu Hospital of Shandong University, Jinan, China.

<sup>9</sup>Brain Science Research Institute, Shandong University, Jinan, China.

<sup>10</sup>Department of Clinical Medicine, University of Bergen, Haukelandsveien 22, 5021 Bergen, Norway.

<sup>11</sup>Turku Centre for Biotechnology, University of Turku and Åbo Akademi University, 20520 Turku, Finland; Department of Pathology, University of Turku, 20520 Turku, Finland.

<sup>12</sup>Department of Biomedicine, University of Bergen, Jonas Lies Vei 91, 5009 Bergen, Norway.

<sup>13</sup>Department of Molecular Medicine; Institute of Basic Medical Sciences; University of Oslo; 0317 Oslo, Norway

<sup>14</sup>Co-first author

<sup>15</sup>Co-senior author

**Short title:** Thioridazine blocks autophagy in glioblastoma cells

**Keywords:** Glioblastoma; temozolomide; drug resistance; thioridazine; autophagy

**Abbreviations used:** Cmap: Connectivity Map; CQ: chloroquine; DRD: dopamine receptor; GBM: glioblastoma multiforme; MGMT: O<sup>6</sup>-methylguanine-methyltransferase; TMZ: temozolomide.

**Corresponding Author:** Lars Prestegarden, Department of Biomedicine, University of Bergen, Jonas Liesvei 91, NO-5009 Bergen, Norway. Tel: +47 55586373; Fax: +47 55586360; E-mail: [Lars.Prestegarden@biomed.uib.no](mailto:Lars.Prestegarden@biomed.uib.no)

This article has been accepted for publication and undergone full peer review but has not been through the copyediting, typesetting, pagination and proofreading process, which may lead to differences between this version and the Version of Record. Please cite this article as doi: 10.1002/ijc.31912

**Conflict of interest:** The authors of this manuscript have no conflicts of interest to declare.

**Word count:** 4302 words excluding references and figure legends

**Total number of figures/tables:** 6 figures

**Article category:** Cancer Therapy and Prevention

**Novelty and Impact:** Resistance to adjuvant temozolomide (TMZ) chemotherapy is the main cause of treatment failure in patients with glioblastoma (GBM) – the most lethal primary brain tumor in adults. Through a genome-wide RNA interference (RNAi) synthetic lethality screen combined with the Connectivity Map database, the authors identified Thioridazine, a dopamine antagonist, as a potent sensitizer of TMZ in GBM cells. Thioridazine blocked the autophagy flux at the autophagosome-lysosome junction, and inhibited tumor growth *in vivo* and increased overall survival in tumor-bearing animals in combination with TMZ. These findings underscore the therapeutic relevance of attenuating autophagy in GBM.

**ABSTRACT**

Glioblastoma multiforme (GBM) has a poor prognosis with an overall survival of 14-15 months following surgery, radiation and chemotherapy using temozolomide (TMZ). A major problem is that the tumors acquire resistance to therapy. In an effort to improve the therapeutic efficacy of TMZ, we performed a genome-wide RNA interference (RNAi) synthetic lethality screen to establish a functional gene signature for TMZ sensitivity in human GBM cells. We then queried the Connectivity Map database to search for drugs that would induce corresponding changes in gene expression. By this approach we identified several potential pharmacological sensitizers to TMZ, where the most potent drug was the established antipsychotic agent Thioridazine, which significantly improved TMZ sensitivity while not demonstrating any significant toxicity alone. Mechanistically, we show that the specific chemosensitizing effect of Thioridazine is mediated by impairing autophagy, thereby preventing adaptive metabolic alterations associated with TMZ resistance. Moreover, we demonstrate that Thioridazine inhibits late-stage autophagy by impairing fusion between autophagosomes and lysosomes. Finally, Thioridazine in combination with TMZ significantly inhibits brain tumor growth *in vivo*, demonstrating the potential clinical benefits of compounds targeting the autophagy-lysosome pathway. Our study emphasizes the feasibility of exploiting drug repurposing for the design of novel therapeutic strategies for GBM.

## INTRODUCTION

Cancer treatment has gradually changed from traditional chemotherapeutics to targeted therapies interfering with key tumor signaling pathways. However, despite some promising results, most treatment responses are short-lived with limited effects on overall survival. No new pharmacological agents have so far been shown to improve outcome for newly diagnosed GBM patients. Current treatment consists of surgical resection followed by radiotherapy (RT) plus concomitant and adjuvant chemotherapy with the alkylating agent temozolomide (TMZ). However, tumors usually recur during or shortly after the initial treatment course, and the median survival time for newly diagnosed GBM patients is only 14-15 months <sup>1</sup>.

Several molecular mechanisms leading to TMZ resistance have been identified. The DNA repair protein O<sup>6</sup>-methylguanine-methyltransferase (MGMT) counteracts TMZ-induced cytotoxicity by restoring the structural integrity of O<sup>6</sup>-alkylated DNA bases <sup>2</sup>. Epigenetic silencing of MGMT expression by promoter hypermethylation has been correlated with improved outcome in GBM patients receiving TMZ <sup>3</sup>. Recent data have also shown that alterations in other DNA repair pathways such as base excision repair (BER) may play a significant role in determining the sensitivity to TMZ <sup>4</sup>. Nevertheless, many tumors that do not express MGMT, or have activation of other known DNA repair pathways, are still resistant to TMZ chemotherapy. Irrespective of the specific genetic alterations leading to drug resistance, a survival strategy common for a wide spectrum of different cancer types is metabolic reprogramming characterized by increased autophagy flux <sup>5,6</sup>.

Results from studies on the role of autophagy in cancer are conflicting. While some reports indicate that increased autophagy flux counteracts malignant progression, others have shown that autophagy represents a survival strategy for cancer cells <sup>7</sup>. However, TMZ and several other chemotherapeutics increase autophagy flux, and the prevailing view is that this supports cancer growth <sup>8-10</sup>. Thus, blocking a GBM survival mechanism such as autophagy could be a potential strategy to kill TMZ-treated GBM cells. Recently a phase I/II clinical trial with the autophagy inhibitor hydroxychloroquine given concomitantly with standard chemoradiotherapy and adjuvant chemotherapy failed to demonstrate a significant benefit for newly diagnosed GBM patients <sup>11</sup>. However, due to toxic side effects proper inhibition of autophagy was not achieved in many patients. As such, new inhibitors with increased

pharmacological properties are needed to address the potential clinical benefit of autophagy inhibition in GBM treatment.

In the present study we show that the established dopamine receptor antagonist Thioridazine is a potent sensitizer of TMZ cytotoxicity. Most notably, we show mechanistically that this effect is independent of dopamine receptor signaling, and that the specific chemosensitizing effect is mediated by impaired late-stage autophagy in GBM cells. Importantly, the combination of Thioridazine and TMZ significantly reduces growth of human intracranial GBM xenografts *in vivo* and prolongs survival in tumor-bearing mice compared to TMZ alone.

## MATERIALS AND METHODS

### shRNA synthetic lethality screen

A genome-wide lentiviral pooled short hairpin RNA (shRNA) screen was performed using a pool of 27,290 shRNAs targeting 5,046 known human genes (Decipher, Human module I, [Cellecta, CA] to identify genes essential for survival during TMZ treatment. Lentiviral vectors were produced as described previously<sup>12</sup>. 40 million U87 GBM cells were infected with the lentiviral library in the presence of 5 µg/ml hexadimethrine bromide (Sigma Aldrich, St. Louis, MO) at MOI of 0.1 ensuring a 5% transfection efficiency. After 3 days, the infected cells were purified by FACS based on the expression of RFP. After sorting, cells were allowed to recover for 1 day before being divided into 3 control populations (serum with 0.1% DMSO) or 3 treatment populations (TMZ, 5.0 µM, 0.5 µM and 0.1 µM). After 10 days of incubation, cells were collected for analysis. Briefly, DNA was extracted and barcodes were PCR amplified before sequencing on Illumina HiSeq (2x10<sup>7</sup> reads) (performed by Cellecta).

### Bioinformatics analysis

Raw data were analyzed using the R language (The R Foundation for Statistical Computing, Vienna, Austria) and shRNAseq, a package developed by ROCK (Institute of Cancer Research, London, <https://stat.ethz.ch/pipermail/bioconductor/2013-November/056100.html>). The vignette at their site was followed with slight modifications. Briefly, the data was log transformed, normalized, and summarized, before each shRNA was given a z-score, where low z-scores represent shRNAs that induce a lower normalized cell count

among the treated group than the controls after silencing. A significant “hit” was defined as any gene that got at least one z-score that was greater than or equal to 2 or less than or equal to -2. This resulted in a list of genes that when silenced, decreased cell viability after treatment with sub-lethal doses of TMZ, and vice versa. This list of genes was integrated into ConnectivityMap build 02 (Cmap) <sup>13, 14</sup>. Cmap is an initiative by the Broad Institute of MIT and Harvard, where the effects of 1,309 small molecules on several cultured human cells have been systematically examined, resulting in a collection of more than 7,000 expression profiles that can be freely queried using their web interface. These have been used successfully in previous studies to select for drugs that produce a disease-negating gene signature <sup>15</sup>. In our case, positively scoring drugs predicted by Cmap would down-regulate genes with negative z-score, and up-regulate genes that decrease high z-score. We thus hypothesized that these drugs would sensitize our cancer cell lines to concurrent TMZ treatment.

#### **Cell lines, tumor material and reagents**

The human glioma cell lines A172, LN18, T98, U87 and U251 were obtained from the American Type Culture Collection (ATCC, Rockville, MA). DNA fingerprinting by short tandem repeat (STR) analysis was performed using AmpFISTR Profiler Plus PCR Amplification Kit (Applied Biosystems, Foster City, CA), and aligned with consensus STR profiles in the ExPASy Bioinformatics Portal (<https://www.expasy.org/>) by using “Cellosaurus”. Cells were maintained in Dulbecco’s Modified Eagle’s Medium (Sigma, St. Louis, MO) supplemented with 10% fetal bovine serum, L-glutamine, non-essential amino acids and antibiotics (100 U/mL penicillin, 100 U/mL streptomycin and  $5 \times 10^{-3}$  mg/mL plasmocin). All cell lines were cultured at 37°C in a 5% CO<sub>2</sub>-humidified atmosphere. Patient GBM-derived spheroids (P3) were expanded through serial transplantation in nude rats, thus generating a standardized pool of spheroids (300–400 µm in diameter) and giving rise to phenotypically identical (highly invasive and highly angiogenic) GBMs in all xenografts <sup>16</sup>. The collection of human biopsy tissue was approved by the regional ethical committee (Haukeland University Hospital, Bergen, Norway). Thioridazine and TMZ were purchased from Tocris Bioscience (Bristol, UK) and dissolved in DMSO to obtain 100 mM stock solutions. Chloroquine was obtained from Sigma, and dissolved in sterile water to obtain a 50 mM stock solution.

### **Identification of drugs and cell viability assays**

Using the U87 human GBM cell line, we screened all commercially available drugs from the top 20 hits (13 drugs) obtained from Cmap. Each drug was tested at incremental doses as monotherapy and as co-treatment with TMZ. Cells were plated in a 96-well format at a concentration of 5000 cells/well and incubated for 96 hours with each drug. Cell viability was assayed using the CellTiter 96 Aqueous One Solution Cell Proliferation Assay (MTS assay, Promega, Madison, WI) according to the manufacturer's instructions. Clonogenic survival assays were basically performed as described previously<sup>17</sup>. Cell proliferation was determined using the trypan blue exclusion assay.

### **Protein extraction and Western blotting**

Protein extraction and western blotting were essentially carried out as described previously<sup>17</sup>. The following primary antibodies were used: anti-MGMT (1:2000; Origene, Rockville, MD), anti-D2DR (1:100; Santa Cruz Biotechnology, CA), anti-GAPDH (1:5000), anti-cleaved-Caspase-3 (1:1000), anti-PARP (1:1000), anti-SQSTM1/p62 (1:1000) and anti-LC3A/B (1:1000) (all from Cell Signaling, Danvers, MA). The secondary antibodies goat anti-mouse IgG-HRP (sc-2005) and goat anti-rabbit IgG-HRP (IM0831) were from Santa Cruz Biotechnology (Santa Cruz, CA) and Beckman Coulter (Marseille, France), respectively.

### **Cell transfection**

To generate stable GBM cell lines devoid of DRD2 expression, lentiviral constructs expressing shRNA-RFP-Puromycin (either containing a scrambled shRNA control or the following DRD2-targeting sequence: ACCGGGCCCTTCTTCATTACACATA TGTTAATATTCATAGCATGTGTGTGATGAAGAAGGGCTTTT) were purchased from Collecta. Silencing of DRD2 expression using the CRISPR-Cas9 technique was performed by using a dual construct containing both Cas9 and sgRNA (target sequence: ACCGGACGATCAGGTAGTTGGTGG) within the same vector (Collecta). Control cells were transfected with empty vector. Briefly, cells were infected with lentiviral particles at 1 MOI in the presence of 5 µg/ml hexadimethrine bromide (Sigma Aldrich, St. Louis, MO) before expansion in puromycin-containing (2 µg/ml) growth medium. Knockdown of DRD2 protein expression in the emerging polyclonal puromycin-resistant populations was validated with western blotting. The

GFP-LC3 plasmid was a kind gift from Drs Yoshimori and Mizushima (Osaka University), and the EGFP-Cherry-LC3 plasmid was a generous gift from Prof. Terje Johansen (University of Tromsø, Norway). Transient over-expression studies of MGMT and DRD2 were performed by using the human expression vector pCMV6-AC containing the corresponding cDNA (Origene). All transfections were carried out using FuGENE® HD Transfection Reagent (Promega) according to the manufacturer's instructions.

### **Transmission electron microscopy**

The electron microscopy sections were prepared as described previously<sup>18</sup>. The area of autophagic vacuoles was measured using "Point Density" plugin for ImageJ (<https://imagej.nih.gov/ij/index.html>). The total area of autophagic vacuoles ( $\mu\text{m}^2$ ) and the total number of autophagic vacuoles in each cell in the Thioridazine (8 $\mu\text{M}$ ) treated group was normalized to the average autophagic area and average number of autophagic vacuoles, respectively, in the control group to calculate fold change between the two groups. At least 100 cells were independently scored in each treatment group.

### **Fluorescence microscopy**

Fluorescent images were obtained with a Zeiss LSM 510 Meta confocal microscope. Images were analyzed with Adobe Photoshop (Adobe Systems) and Imaris (Bitplane, MA, USA). LysoTracker Red DND-99 (Life Technologies) was used according to the manufacturer's instructions for visualization of lysosomes. Briefly, cells were treated with either drug vehicle or Thioridazine for 24 hrs, and then incubated with 50 nM LysoTracker dye for 1 h at 37°C before examination under the fluorescence microscope. All images were pseudocoloured green. LysoTracker labeling was also quantified in the different treatment groups using an Accuri C6 flow cytometer (BD Biosciences, San Jose, CA).

### **Animal experiments**

10  $\mu\text{L}$  of cell suspension containing a total of  $1 \times 10^6$  cells (first animal cohort) or five human GBM spheroids (second animal cohort) were stereotactically implanted into the brain (1 mm posterior to the bregma and 2 mm to the right of the midline suture at a depth of 1.5 mm) of NOD/SCID mice. All animal procedures were approved by the



National Animal Research Authority in Norway. After 10 days, the animals were stratified into the following groups: drug vehicle, Thioridazine (20 mg/kg), TMZ (20 mg/kg) and Thioridazine + TMZ (20 mg/kg + 20 mg/kg). Treatment was administered 3 times the first week and daily for the following 3 weeks by intraperitoneal injection. After 6 weeks, mice in the second cohort study underwent MRI scans (with and without contrast) weekly to monitor tumor growth kinetics. Animals were sacrificed at the onset of symptoms using CO<sub>2</sub>. Tumors were removed and either formaline fixed for histology or snap frozen in liquid N<sub>2</sub> for further studies. All mice treated with Thioridazine developed transient symptoms of drowsiness. However, these symptoms improved during the treatment.

### **MR imaging**

MRI was performed on a 7T Pharmascan (Bruker, Ettlingen, Germany). Sequence details have been described previously<sup>19</sup>. We performed brain MRI to evaluate tumor growth with pre-/post-contrast T1-weighted sequences.

### **Statistical analyses**

Data are presented as mean  $\pm$  SEMs of 3 independent experiments. Statistical analyses were carried out using a two-tailed Student's t-test assuming equal variances. When multiple groups were evaluated, the one-way ANOVA test with post-hoc Turkey-Kramer multiple comparisons test was used.  $P < 0.05$  was considered statistically significant.

## **RESULTS**

### **Identification of chemosensitizing compounds**

We first transfected the human GBM cell line U87 with a pooled lentiviral shRNA library targeting 5,046 genes, and incubated the cells at three sub-lethal TMZ concentrations or in control medium containing drug vehicle only. A schematic outline of the synthetic lethality screen is shown in Fig. 1A. Individual silencing of 292 genes lead to a significantly reduced cell growth in the TMZ-treated population compared to the control group (Supplementary table 1). To identify known drugs that could similarly down-regulate these gene clusters, we interrogated the Connectivity Map (Cmap) database (<https://www.broadinstitute.org/cmap/>). A number of compounds with potential cytotoxic activity were identified. Upon validation in low-

throughput cell viability assays, we found that some compounds had no therapeutic effect, whereas others, such as the anti-psychotic agent Thioridazine, the phytoestrogen Resveratrol and the antibiotic Furazolidone showed a synergistic effect with concomitant TMZ therapy (Fig. 1B). However, only Thioridazine (Fig. 1C) met all criteria for our study: 1) no significant cytotoxicity when given as low-dose monotherapy 2) adequate pharmacological properties for targeting intracranial tumors and 3) synergistic cytotoxic effect with TMZ.

To confirm our initial observations identifying Thioridazine as a TMZ chemosensitizer, we expanded our study using a panel of GBM cell lines with different genetic backgrounds. Importantly, whereas Thioridazine alone had little or no cytotoxic activity, the combination of Thioridazine and TMZ had a profound cytotoxic effect on all the examined glioma cell lines (Fig. 1D). This was also seen in the TMZ resistant cell line T98 that expresses the DNA repair protein MGMT, and which also harbors a *TP53* missense mutation<sup>20</sup>. To corroborate our findings from the cell viability assay, we next performed clonogenic survival assays for U87 (MGMT deficient), LN18 and T98 cells (the latter two cell lines expressing MGMT) in response to TMZ/Thioridazine. Notably, the combination of TMZ and Thioridazine resulted in a significant decrease in clonogenicity as a measure of cellular survivability in both the MGMT deficient and -proficient cell lines compared to either agent alone (Fig. 1E).

In summary, our results show that the phenothiazine Thioridazine in single-digit micromolar concentrations is a potent sensitizer of GBM cells to TMZ chemotherapy *in vitro*.

### **Thioridazine improves TMZ cytotoxicity independently of MGMT expression**

Having observed that the combination of Thioridazine and TMZ significantly decreases cell viability compared to either agent alone in a panel of established GBM cell lines, we next examined whether MGMT expression would impact the effect of Thioridazine, TMZ or both agents combined. As shown in Fig. 2A, only LN18 and T98G expressed MGMT at the protein level, whereas A172, U87 and U251 showed no detectable expression of MGMT protein. Transfected U87 cells overexpressing MGMT (Fig. 2B) were significantly more resistant to TMZ compared to syngeneic control cells (Fig. 2C). However, MGMT expression did not influence the therapeutic efficacy of Thioridazine alone or the combination of Thioridazine and TMZ. This was

in agreement with our initial observation in Fig. 1D where Thioridazine could enhance TMZ cytotoxicity equally well in both MGMT proficient and – deficient GBM cells. Based on these results, we conclude that MGMT expression does not counteract the chemosensitizing effect of Thioridazine, and suggest that this potential therapeutic strategy could be employed in GBM cells irrespective of MGMT expression status.

### **The chemosensitizing effect of Thioridazine is dopamine receptor independent**

To interrogate the mechanisms involved during Thioridazine treatment, we initially scrutinized the potential inhibitory effect of Thioridazine towards the dopamine receptors (DRDs). These receptors are G-protein coupled receptors (GPCRs) mainly expressed in the central nervous system. The D1-like receptors (DRD1 and DRD5) are in general excitatory while the D2-like receptors (DRD2-DRD4) are inhibitory<sup>21</sup>. Thioridazine inhibits the signaling activity of the D2-like dopamine receptors with highest affinity towards DRD2<sup>22</sup>. We therefore evaluated the expression of DRD2 in our panel of GBM cell lines. Notably, among the cell lines that were sensitized to TMZ by concurrent treatment with Thioridazine, only LN18 expressed any detectable levels of DRD2 protein (Fig. 3A). This finding led us to hypothesize that Thioridazine exerts its chemosensitizing effect in GBM cells independently of any DRD2 expression. To test this hypothesis, we silenced DRD2 expression in LN18 using CRISPR-Cas9 and shRNA constructs before treatment with Thioridazine and TMZ. Both approaches significantly lowered DRD2 expression in LN18 cells (Fig. 3B) compared to cells transfected with control sgRNA. However, decreased DRD2 levels did not impact the cellular response to Thioridazine, TMZ or both agents combined (Fig. 3C), suggesting that Thioridazine could potentiate TMZ cytotoxicity independently of its function as a DRD2 inhibitor. To further corroborate that DRD2 expression was not crucial for the chemosensitizing effect of Thioridazine, we overexpressed DRD2 in U87 cells (Fig. 3D), which initially showed no detectable DRD2 protein expression. As expected, we could not observe any significant change in response to Thioridazine or TMZ in U87-DRD2 expressing cells (Fig. 3E).

Taken together, our findings demonstrate that DRD2 expression does not modulate Thioridazine or TMZ sensitivity in GBM cells, and that Thioridazine improves TMZ cytotoxicity regardless of any DRD2 expression.

### Thioridazine impairs autophagy

Thioridazine has previously been shown to decrease cellular inhibitors of apoptosis protein (IAP) expression levels and consequently induce apoptosis in ovarian xenografts *in vivo*<sup>23</sup>. However, we could not detect any cleavage of Caspase 3 or PARP in cells treated with Thioridazine or the combination of Thioridazine and TMZ (Suppl. Fig. 1A). Furthermore, co-treatment with the pan-caspase inhibitor z-VAD-fmk did not abrogate the increased TMZ cytotoxicity caused by Thioridazine (Suppl. Fig. 1B). These findings indicate that Thioridazine treatment together with TMZ modulates cell survival in GBM cells by another mechanism than apoptosis.

During the experiments, we observed that low-dose Thioridazine treatment leads to an accumulation of perinuclear vacuoles (Fig. 4A). Thus, we hypothesized that this could represent an alteration in autophagy. To address this question, U87 cells were transfected with a plasmid expressing a GFP-LC3 fusion protein prior to treatment with Thioridazine. As shown in Fig. 4B and C, there was a significant increase in the number of cells displaying GFP-LC3-positive puncta after Thioridazine treatment compared to control cells, indicating an accumulation of autophagosomes. To further determine whether the observed formation of autophagosomes caused by Thioridazine reflected an increased autophagy flux or blockade of autophagosome turnover, we studied the expression of LC3A/B-I and LC3A/B-II as well as the polyubiquitin-binding protein p62/SQSTM1 in U87 cells treated with TMZ, Thioridazine or both compounds combined. In agreement with induction of autophagy, TMZ caused increased formation of LC3A/B-II whereas levels of p62, which normally is consumed during autophagic degradation, were diminished (Fig. 4D). In contrast, Thioridazine exposure was associated with increased formation of LC3A/B-II, and significant accumulation of p62, suggesting inhibition of autophagy. Finally, p62 levels accumulated as well in cells treated with TMZ plus Thioridazine. Taken together, our findings demonstrate that Thioridazine leads to inhibition of autophagy and the subsequent accumulation of autophagosomes in GBM cells.

To assess whether the observed inhibition of autophagy occurred due to impaired fusion between autophagosomes and lysosomes, we transfected U87 cells with a tandem EGFP-Cherry-LC3 plasmid. EGFP fluorescence is unstable and quenched in the acid environment of the lysosomes/autophagolysosomes. As such, if the autophagosomes are able to fuse with the lysosomes, the green fluorescence will

be reduced making the red fluorescence predominant. As shown in Suppl. Fig. 2A, there was no reduction in GFP-positive puncta during treatment with Thioridazine. These observations were similar to results from treatment with the established lysosome inhibitor Bafilomycin A1, which was used as a positive control. However, upon treatment with Rapamycin, an inducer of autophagy, there was an accumulation of only red puncta. Collectively, these results indicate an accumulation of autophagosomes that are unable to fuse with the lysosomes. To further substantiate these findings, we investigated the ultrastructural alterations in U87 cells following treatment with Thioridazine using transmission electron microscopy (TEM). Untreated U87 cells only displayed a few scattered autophagosome vacuoles (AV) while Thioridazine treated cells displayed a considerable accumulation of large double-membrane AVs throughout the cytoplasm (Fig 4E and F). Finally, LysoTracker labeling showed significantly decreased formation of acidic vesicular organelles in response to Thioridazine (Fig. 4G and 4H), indicating compromised acidification of lysosomes.

To provide evidence that pharmacological blockade of late-stage autophagy could serve as a novel strategy in concert with chemotherapy, we also studied whether the established autophagy inhibitors chloroquine (CQ) and Bafilomycin A1 would improve TMZ cytotoxicity in GBM cells. These compounds are recognized for their ability to prevent maturation of autophagic vacuoles by inhibiting fusion between autophagosomes and lysosomes through neutralization of lysosomal pH. As demonstrated in Fig. 4I, both CQ and Bafilomycin A1 in combination with TMZ significantly reduced cell viability compared to either agent alone, although CQ was associated with some degree of cytotoxicity as monotherapy. Overall, our results show that Thioridazine is an efficient inhibitor of late-stage autophagy by preventing the fusion between autophagosomes and lysosomes, and that targeting of the autophagic flux, together with TMZ chemotherapy, constitutes a promising therapeutic approach in GBM cells in general.

### **Temozolomide in combination with Thioridazine significantly decreases growth of orthotopic glioma xenografts *in vivo***

The therapeutic efficacy of combining TMZ and Thioridazine was further studied *in vivo* in NOD/SCID mice carrying orthotopically implanted U87 xenografts. Ten days subsequent to implantation, the mice were randomized to one of the four treatment

groups consisting of drug vehicle (n=10), Thioridazine (20 mg/kg; n=10), TMZ (20 mg/kg; n=10) or TMZ plus Thioridazine (20 mg/kg + 20 mg/kg; n=10). Treatment with Thioridazine monotherapy at this concentration did not improve survival in tumor bearing animals compared to the control group (Fig. 5A). In contrast, TMZ alone significantly delayed tumor growth and improved survival compared to animals receiving drug vehicle, consistent with the fact that TMZ is a clinically active drug against GBM. Importantly, the combination of TMZ and Thioridazine significantly extended animal survival compared to either agent alone, consistent with our findings *in vitro* showing that Thioridazine increases TMZ sensitivity in GBM cells.

To further substantiate our results identifying Thioridazine as a promising chemosensitizing agent *in vivo*, we initiated a second cohort study using highly characterized patient-derived GBM spheroids<sup>18</sup>. This study was also expanded to include weekly MRI scans from week six to determine tumor growth in response to the different treatments, and the tumor volume for each animal (n=5 for each group) was calculated from the obtained MRI at each time point. In agreement with our findings from the initial *in vivo* study, TMZ significantly decreased tumor growth compared to animals receiving drug vehicle (Fig. 5B and 5C). However, the combination of TMZ and Thioridazine led to a more pronounced decrease in tumor growth compared to controls and animals treated with TMZ alone (Figure 5B and C). The observed delays in tumor growth caused by TMZ alone and TMZ plus Thioridazine also translated into improved outcome compared to animals treated with drug vehicle (Fig. 5D). Notably, the addition of Thioridazine to TMZ significantly extended overall survival compared to TMZ alone.

In summary, our findings using a clinically relevant orthotopic xenograft model confirm that Thioridazine acts as a potent sensitizer for TMZ chemotherapy *in vivo* with the potential for reducing tumor burden and prolonging survival.

## DISCUSSION

The role of autophagy in cancer is controversial and the literature is conflicting<sup>24</sup>. Animal studies have demonstrated that defects in autophagy are associated with increased susceptibility of cancer, which has indicated a tumor suppressor function for autophagy<sup>25</sup>. However, a large number of studies show that autophagy supports cancer cell survival<sup>26, 27</sup>, especially under adverse conditions with an increased demand for metabolic activity<sup>7</sup>. In the present study we demonstrate that autophagy

promotes GBM cell survival during TMZ chemotherapy. These findings support previous results where inhibition of autophagy synergized with chemotherapy<sup>9</sup>. The specific mechanism in which Thioridazine leads to abortive autophagy<sup>28</sup> is likely due to its biochemical properties, which has been thoroughly elucidated previously. Thioridazine is a base with pKa of 9,5 and accumulates in lysosomes by lysosomal trapping<sup>29</sup>, giving a lysosome/cytosol concentration ratio of about 75 in some cells<sup>30</sup>. This attenuates lysosome function by pH partitioning and inhibits fusion with autophagosomes<sup>31</sup>.

Several other compounds like hydroxychloroquine and Bafilomycin A1 inhibits late stage autophagy. However, due to its high lipophilicity Thioridazine accumulates in the brain<sup>32</sup> making it an ideal compound for targeting intracranial malignancies. Furthermore, Thioridazine has been used in the clinic since the early 1950s. As such, the toxicity profile is well known, indicating that autophagy directed therapy is well tolerated. Previous clinical trials with inhibitors of autophagy (e.g. hydroxychloroquine) have been hampered with off-target dose limiting effects, and proper inhibition of autophagy has consequently not been achieved<sup>11, 33</sup>. Thus, Thioridazine-derivatives might be promising drug candidates for targeting autophagy in GBMs due to its low toxicity and its ability to cross the blood-brain-barrier.

In summary, this study demonstrates the feasibility of linking results from large-scale genome-wide RNAi studies with corresponding drug-induced alterations in gene expression within the Connectivity Map framework. As such, this represents a high-throughput method for drug repositioning. Thioridazine was found to be a potent sensitizer of TMZ chemotherapy in GBM, an effect mediated by impaired late-stage autophagy. Most importantly, this mechanistic synergy conferred significantly reduced tumor growth and increased survival in GBM xenografts *in vivo*. Conclusively, our results strongly encourage further assessment of combined TMZ and Thioridazine treatment in an adjuvant clinical setting.

## ACKNOWLEDGMENTS

**Author contributions:** LP and RB designed the project; TCJ, MMH, HZ, OD, AG, HS, BJ, TS, JV, NY, AN, GR, ML and LP performed research; LP, TCJ, MMH, OD, AG, HS, HZ, BJ, TS, JV, JW, KJT, MLJ, AS, JW and RB analyzed data; and TCJ, RB and LP wrote the paper. All authors approved the final manuscript.

**Financial support:** This work was supported in part by the Kristian Gerhard Jebsen Foundation, the Norwegian Cancer Society, the Norwegian Research Council, Helse Vest, Haukeland University Hospital, the Bergen Medical Research Foundation (all to R. Bjerkvig), and Jane and Aatos Erkko Foundation (to J. Westermarck). Support was also provided by the University of Bergen and Centre de Recherche Public de la Santé through a grant from the Ministry of Research and Higher Education in Luxembourg (to R. Bjerkvig and B. Janji) and the Qilu Hospital of Shandong University through the Special Fund for Taishan Scholarship (to J. Wang).



## REFERENCES

1. Stupp R, Mason WP, van den Bent MJ, Weller M, Fisher B, Taphoorn MJ, Belanger K, Brandes AA, Marosi C, Bogdahn U, Curschmann J, Janzer RC, et al. Radiotherapy plus concomitant and adjuvant temozolomide for glioblastoma. *The New England journal of medicine* 2005;352:987-96.
2. Hegi ME, Diserens AC, Godard S, Dietrich PY, Regli L, Ostermann S, Otten P, Van Melle G, de Tribolet N, Stupp R. Clinical trial substantiates the predictive value of O-6-methylguanine-DNA methyltransferase promoter methylation in glioblastoma patients treated with temozolomide. *Clinical cancer research : an official journal of the American Association for Cancer Research* 2004;10:1871-4.
3. Gorlia T, van den Bent MJ, Hegi ME, Mirimanoff RO, Weller M, Cairncross JG, Eisenhauer E, Belanger K, Brandes AA, Allgeier A, Lacombe D, Stupp R. Nomograms for predicting survival of patients with newly diagnosed glioblastoma: prognostic factor analysis of EORTC and NCIC trial 26981-22981/CE.3. *The Lancet. Oncology* 2008;9:29-38.
4. Agnihotri S, Burrell K, Buczkowicz P, Remke M, Golbourn B, Chornenkyy Y, Gajadhar A, Fernandez NA, Clarke ID, Barszczyk MS, Pajovic S, Ternamian C, et al. ATM regulates 3-methylpurine-DNA glycosylase and promotes therapeutic resistance to alkylating agents. *Cancer discovery* 2014;4:1198-213.
5. Perera RM, Stoykova S, Nicolay BN, Ross KN, Fitamant J, Boukhali M, Lengrand J, Deshpande V, Selig MK, Ferrone CR, Settleman J, Stephanopoulos G, et al. Transcriptional control of autophagy-lysosome function drives pancreatic cancer metabolism. *Nature* 2015.
6. Gopal YN, Rizos H, Chen G, Deng W, Frederick DT, Cooper ZA, Scolyer RA, Pupo G, Komurov K, Sehgal V, Zhang J, Patel L, et al. Inhibition of mTORC1/2 overcomes resistance to MAPK pathway inhibitors mediated by PGC1alpha and oxidative phosphorylation in melanoma. *Cancer research* 2014;74:7037-47.
7. Degenhardt K, Mathew R, Beaudoin B, Bray K, Anderson D, Chen G, Mukherjee C, Shi Y, Gelinas C, Fan Y, Nelson DA, Jin S, et al. Autophagy promotes tumor cell survival and restricts necrosis, inflammation, and tumorigenesis. *Cancer cell* 2006;10:51-64.
8. Natsumeda M, Aoki H, Miyahara H, Yajima N, Uzuka T, Toyoshima Y, Kakita A, Takahashi H, Fujii Y. Induction of autophagy in temozolomide treated malignant gliomas. *Neuropathology : official journal of the Japanese Society of Neuropathology* 2011;31:486-93.
9. Amaravadi RK, Yu D, Lum JJ, Bui T, Christophorou MA, Evan GI, Thomas-Tikhonenko A, Thompson CB. Autophagy inhibition enhances therapy-induced apoptosis in a Myc-induced model of lymphoma. *The Journal of clinical investigation* 2007;117:326-36.
10. Kenific CM, Debnath J. Cellular and metabolic functions for autophagy in cancer cells. *Trends in cell biology* 2015;25:37-45.
11. Rosenfeld MR, Ye X, Supko JG, Desideri S, Grossman SA, Brem S, Mikkelsen T, Wang D, Chang YC, Hu J, McAfee Q, Fisher J, et al. A phase I/II trial of hydroxychloroquine in conjunction with radiation therapy and concurrent and adjuvant temozolomide in patients with newly diagnosed glioblastoma multiforme. *Autophagy* 2014;10:1359-68.

12. Prestegarden L, Svendsen A, Wang J, Sleire L, Skaftnesmo KO, Bjerkvig R, Yan T, Askland L, Persson A, Sakariassen PO, Enger PO. Glioma cell populations grouped by different cell type markers drive brain tumor growth. *Cancer research* 2010;70:4274-9.
13. Lamb J. The Connectivity Map: a new tool for biomedical research. *Nature reviews. Cancer* 2007;7:54-60.
14. Lamb J, Crawford ED, Peck D, Modell JW, Blat IC, Wrobel MJ, Lerner J, Brunet JP, Subramanian A, Ross KN, Reich M, Hieronymus H, et al. The Connectivity Map: using gene-expression signatures to connect small molecules, genes, and disease. *Science* 2006;313:1929-35.
15. Qu XA, Rajpal DK. Applications of Connectivity Map in drug discovery and development. *Drug discovery today* 2012;17:1289-98.
16. Wang J, Miletic H, Sakariassen PO, Huszthy PC, Jacobsen H, Brekka N, Li X, Zhao P, Mork S, Chekenya M, Bjerkvig R, Enger PO. A reproducible brain tumour model established from human glioblastoma biopsies. *BMC cancer* 2009;9:465.
17. Johannessen TC, Prestegarden L, Grudic A, Hegi ME, Tysnes BB, Bjerkvig R. The DNA repair protein ALKBH2 mediates temozolomide resistance in human glioblastoma cells. *Neuro Oncol* 2013;15:269-78.
18. Sakariassen PO, Prestegarden L, Wang J, Skaftnesmo KO, Mahesparan R, Molthoff C, Sminia P, Sundlisaeter E, Misra A, Tysnes BB, Chekenya M, Peters H, et al. Angiogenesis-independent tumor growth mediated by stem-like cancer cells. *Proceedings of the National Academy of Sciences of the United States of America* 2006;103:16466-71.
19. Sundstrom T, Daphu I, Wendelbo I, Hodneland E, Lundervold A, Immervoll H, Skaftnesmo KO, Babic M, Jendelova P, Sykova E, Lund-Johansen M, Bjerkvig R, et al. Automated tracking of nanoparticle-labeled melanoma cells improves the predictive power of a brain metastasis model. *Cancer research* 2013;73:2445-56.
20. Quick QA, Gewirtz DA. An accelerated senescence response to radiation in wild-type p53 glioblastoma multiforme cells. *Journal of neurosurgery* 2006;105:111-8.
21. Keeler JF, Pretsell DO, Robbins TW. Functional implications of dopamine D1 vs. D2 receptors: A 'prepare and select' model of the striatal direct vs. indirect pathways. *Neuroscience* 2014;282C:156-75.
22. Roth BD, J. Psychoactive Drug Screening Program (PDSP). PDSP Ki Database 2011.
23. Park MS, Dong SM, Kim BR, Seo SH, Kang S, Lee EJ, Lee SH, Rho SB. Thioridazine inhibits angiogenesis and tumor growth by targeting the VEGFR-2/PI3K/mTOR pathway in ovarian cancer xenografts. *Oncotarget* 2014;5:4929-34.
24. Yang ZJ, Chee CE, Huang S, Sinicrope FA. The role of autophagy in cancer: therapeutic implications. *Molecular cancer therapeutics* 2011;10:1533-41.
25. Qu X, Yu J, Bhagat G, Furuya N, Hibshoosh H, Troxel A, Rosen J, Eskelinen EL, Mizushima N, Ohsumi Y, Cattoretti G, Levine B. Promotion of tumorigenesis by heterozygous disruption of the beclin 1 autophagy gene. *The Journal of clinical investigation* 2003;112:1809-20.
26. Yang S, Wang X, Contino G, Liesa M, Sahin E, Ying H, Bause A, Li Y, Stommel JM, Dell'antonio G, Mautner J, Tonon G, et al. Pancreatic cancers require autophagy for tumor growth. *Genes & development* 2011;25:717-29.

27. Guo JY, Chen HY, Mathew R, Fan J, Strohecker AM, Karsli-Uzunbas G, Kamphorst JJ, Chen G, Lemons JM, Karantza V, Collier HA, D'Paola RS, et al. Activated Ras requires autophagy to maintain oxidative metabolism and tumorigenesis. *Genes & development* 2011;25:460-70.
28. Wojtkowiak JW, Sane KM, Kleinman M, Sloane BF, Reiners JJ, Jr., Mattingly RR. Aborted autophagy and nonapoptotic death induced by farnesyl transferase inhibitor and lovastatin. *J Pharmacol Exp Ther* 2011;337:65-74.
29. Daniel et al WA. The role of lysosomes in the cellular distribution of thioridazine and potential drug interactions. *Toxicology and applied pharmacology* 1999;158:115-24.
30. Hammarlund-Udenaes. *Drug Delivery to the Brain: Physiological Concepts, Methodologies and Approaches* 2014;2210-7371.
31. Ashoor R, Yafawi R, Jessen B, Lu S. The contribution of lysosomotropism to autophagy perturbation. *PloS one* 2013;8:e82481.
32. Daniel WA. Mechanisms of cellular distribution of psychotropic drugs. Significance for drug action and interactions. *Progress in neuro-psychopharmacology & biological psychiatry* 2003;27:65-73.
33. McAfee Q, Zhang Z, Samanta A, Levi SM, Ma XH, Piao S, Lynch JP, Uehara T, Sepulveda AR, Davis LE, Winkler JD, Amaravadi RK. Autophagy inhibitor Lys05 has single-agent antitumor activity and reproduces the phenotype of a genetic autophagy deficiency. *Proceedings of the National Academy of Sciences of the United States of America* 2012;109:8253-8.

## Figure legends

### Figure 1.

**A genome-wide shRNA synthetic lethality screen identifies Thioridazine as a potent sensitizer of TMZ cytotoxicity.**

(A) Overall experimental design. Gene hits from the high-throughput RNAi screen in U87 cells were used to interrogate the Connectivity Map database to identify potential pharmacological sensitizers to TMZ chemotherapy.

(B) Identification of drugs potentiating the cytotoxic effect of TMZ. From the top 20 drug hits, 13 compounds were commercially available and subsequently validated in low-throughput cytotoxicity assays *in vitro*. Each compound was tested as monotherapy and in combination with 100  $\mu$ M TMZ. The figure shows cell viability in response to TMZ (left bar), the identified compound (middle bar) and the combination (right bar) after 96 hours of drug treatment. 6  $\mu$ M Thioridazine, 100  $\mu$ M Resveratrol, 100  $\mu$ M Sulfafurazole and 50  $\mu$ M Furazolidone significantly decreased cell viability when combined with TMZ compared to monotherapy or TMZ alone. The following concentrations are shown for the remaining compounds that did not successfully enhance TMZ cytotoxicity: 100 nM Digitoxigenin, 60 nM Digoxin, 100  $\mu$ M Biperiden, 80 nM Lanatoside C, 200  $\mu$ M Ganciclovir, 100  $\mu$ M Meropenem, 100 nM Strophantidin, 50  $\mu$ M MG-262, and 40 nM Ouabain.

(C) Molecular structure of Thioridazine.

(D) Cell viability assays demonstrating the response of different established GBM cell lines to 100  $\mu$ M TMZ, 6  $\mu$ M Thioridazine, and the combination of 100  $\mu$ M TMZ and 6  $\mu$ M Thioridazine after 96 hours.

(E) Clonogenic assays as a measure of cellular survivability of TMZ sensitive (U87) and -resistant (LN18 and T98) GBM cells in response to TMZ, Thioridazine and the combination of TMZ and Thioridazine. U87 cells were treated with 20  $\mu$ M TMZ, whereas LN18 and T98 cells received 100  $\mu$ M TMZ. All three cell lines were treated with 2  $\mu$ M Thioridazine either alone or in combination with TMZ.

Data are shown as mean  $\pm$  SEMs of 3 independent experiments. \* $P$ <0.05, \*\* $P$ <0.01, \*\*\* $P$ <0.001.

**Figure 2.****MGMT expression does not compromise the increased TMZ sensitivity mediated by Thioridazine**

(A) Western blotting of whole-cell protein lysates demonstrating detectable MGMT expression in LN18 and T98 cells.

(B) Validation of MGMT expression in U87 cells transfected with a mammalian expression vector encoding MGMT cDNA compared to corresponding parental cells. T98 cells were used as a positive control for MGMT expression.

(C) Cell viability assays showing the response of U87 cells expressing MGMT and corresponding parental cells to increasing concentrations of TMZ and (D) response to 100  $\mu$ M, 6  $\mu$ M Thioridazine and the combination of 100  $\mu$ M TMZ and 6  $\mu$ M Thioridazine after 96 hours of drug exposure.

Data are presented as mean  $\pm$  SEMs of 3 independent experiments.

N.S.; not statistically significant, \* $P$ <0.05, \*\* $P$ <0.01, \*\*\* $P$ <0.001.

**Figure 3.****Thioridazine improves TMZ sensitivity in glioma cells irrespective of dopamine receptor 2 (DRD2) expression**

(A) DRD2 expression in five established GBM cell lines determined by western blotting. Only LN18 cells significantly expressed DRD2 at the protein level.

(B) Western blot showing stable downregulation of DRD2 expression in LN18 cells using CRISPR-Cas9 and shRNA-targeting strategies. Control cells were infected with an equivalent scrambled vector encoding only genes for antibiotic selection. Numbers indicate each DRD2 band intensity normalized to its respective GAPDH band.

(C) Viability assays of LN18 cells with established downregulation of DRD2 expression (either by CRISPR-Cas9 or shRNA) and corresponding parental cells treated with 100  $\mu$ M TMZ, 6  $\mu$ M Thioridazine or the combination of 100  $\mu$ M TMZ and 6  $\mu$ M Thioridazine for 96 hours.

(D) Confirmation of DRD2 expression in U87 cells transfected with a mammalian expression vector encoding DRD2 cDNA. Corresponding parental U87 cells did not show detectable levels of DRD2 protein. Protein lysate from LN18 cells was used as a positive control for DRD2 expression.

(E) Viability assays of U87 cells either deficient or proficient in DRD2 expression (as shown in [D]) after treatment with 100  $\mu$ M TMZ, 6  $\mu$ M Thioridazine or the combination of 100  $\mu$ M TMZ and 6  $\mu$ M Thioridazine.

Data are presented as mean  $\pm$  SEMs of 3 independent experiments

\* $P$ <0.05, \*\* $P$ <0.01, \*\*\* $P$ <0.001.

#### Figure 4.

##### Thioridazine decreases cancer cell viability by inhibition of autophagy

(A) Bright field microscopy showing accumulation of perinuclear vacuoles in U87 cells after incubation with 8  $\mu$ M Thioridazine for 24 hrs.

(B) LC3 is accumulated in perinuclear vacuoles (indicated by arrowheads) upon Thioridazine exposure (middle). Cells were transfected with a GFP-LC3 fusion plasmid, and incubated for 24 hours with drug vehicle (control shown on the left) or 8  $\mu$ M Thioridazine (middle and right panel) before visualization of GFP-LC3 expression under a fluorescence microscope. Scale bar = 50  $\mu$ m.

(C) Quantification of U87 cells displaying GFP-puncta as a measure of accumulating LC3-containing perinuclear vacuoles after treatment of 8  $\mu$ M Thioridazine for 24 hours. Cells were considered GFP-positive if they displayed  $\geq 10$  GFP-LC3 puncta.

(D) TMZ and Thioridazine induces accumulation of LCA/B3-II in U87 cells. Whereas p62 levels were decreased in cells receiving TMZ, indicating induction of autophagy, Thioridazine caused accumulation of p62. Cells were treated with either drug vehicle, 100  $\mu$ M TMZ, 8  $\mu$ M Thioridazine or the combination of TMZ and Thioridazine for 24 hours before cell lysates were collected for western blotting.

(E) Representative transmission electron micrographs (TEM) show accumulation of autophagosomes upon Thioridazine exposure. U87 cells were treated with either vehicle (left) or 8  $\mu$ M Thioridazine for 24 hrs before visualization with TEM.

(F) Quantification of autophagosomes in U87 cells treated with drug vehicle or 8  $\mu$ M Thioridazine for 24 hrs based on TEMs as shown in (E).

(G) Fluorescent microscopy using LysoTracker labeling as a measure of lysosomal formation in U87 cells receiving either drug vehicle or 8 $\mu$ M Thioridazine for 24 hrs.

(H) Quantification of LysoTracker labeling in U87 cells by flow cytometry showing decreased formation of lysosomes upon 8 $\mu$ M Thioridazine exposure for 24 hrs compared to control cells.

(I) The established autophagy inhibitors CQ (left panel) and Bafilomycin A1 (right panel) improves TMZ cytotoxicity in U87 cells. Cells were treated with the indicated drug concentrations for 96 hrs before cell viability was determined. Data are presented as mean  $\pm$  SEMs of 3 independent experiments

\* $P < 0.05$ , \*\* $P < 0.01$ , \*\*\* $P < 0.001$ .

### Figure 5.

#### **Temozolomide in combination with Thioridazine significantly inhibits growth of orthotopic glioma xenografts**

(A) Kaplan-Meier survival curves showing significantly prolonged survival of mice with orthotopic U87 xenografts when treated with the combination of TMZ and Thioridazine compared to either agent alone.

(B) Representative T1-weighted coronal brain MRI sections at week 11 of animals with orthotopic patient-derived glioblastoma xenografts treated with PBS, TMZ or the combination of TMZ and Thioridazine. The MRI sections demonstrate significantly reduced tumor burden and less peritumoral edema in animals receiving TMZ plus Thioridazine (right panel) compared to TMZ alone (middle panel) or PBS (left panel).

(C) Quantification of tumor volume ( $\text{mm}^3$ ) in the different treatment groups in (B) based on MRI of all study animals obtained at the indicated time points showing most pronounced reduction in tumor growth in animals treated with TMZ and Thioridazine. Data are expressed as mean  $\pm$  SD.

(D) Kaplan-Meier plots showing significantly improved overall survival of mice bearing patient-derived GBM xenografts treated with TMZ and Thioridazine compared to other treatment groups.

\* $P < 0.05$ , \*\* $P < 0.01$ , \*\*\* $P < 0.001$ .

### Figure 6.

#### **Suggested mechanism of action by Thioridazine in human GBM cells**

In response to TMZ chemotherapy, GBM cells can undergo autophagy in which cellular constituents are degraded and reused in a well-organized manner as part of an adaptive survival process. We suggest that Thioridazine, by blocking the fusion between mature autophagosomes and lysosomes, counteracts this survival mechanism and consequently improves TMZ cytotoxicity and cell death.

Figure 1

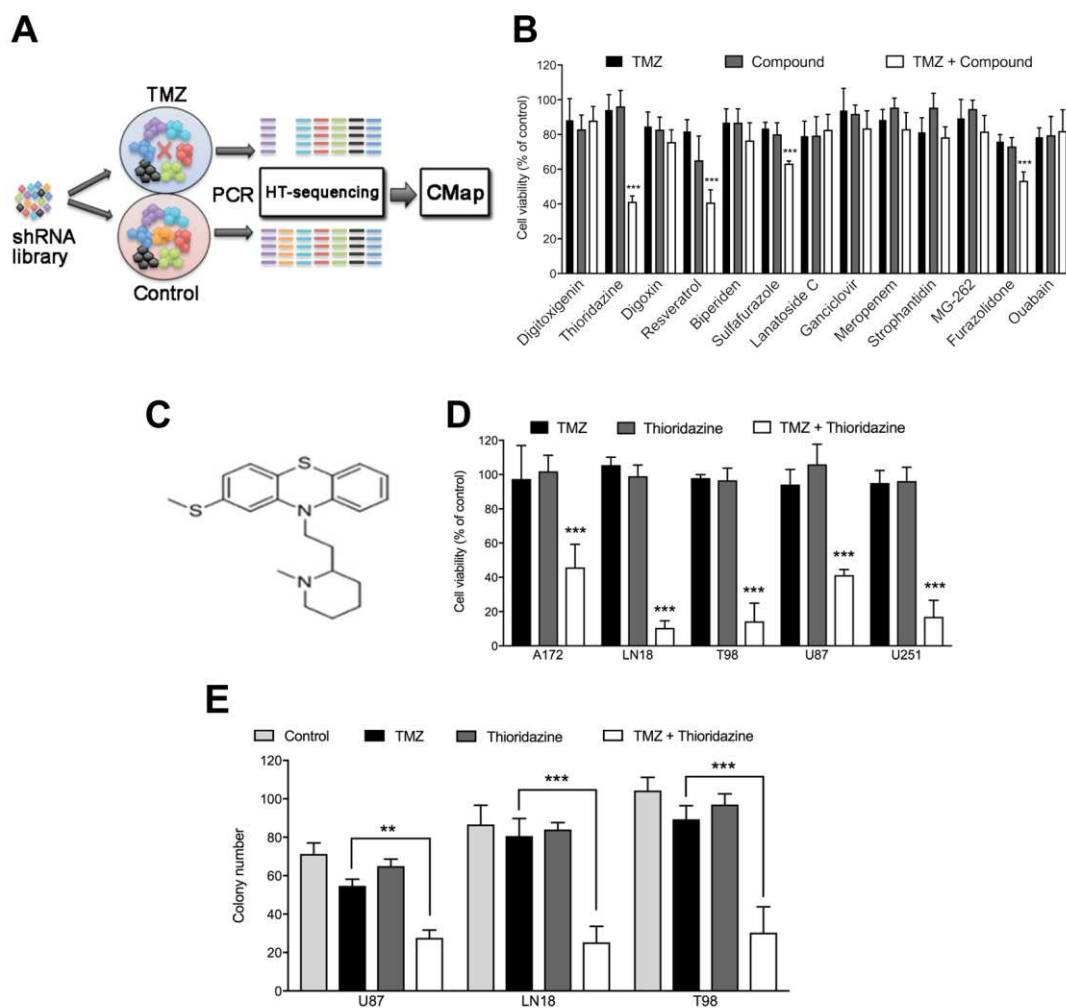




Figure 2

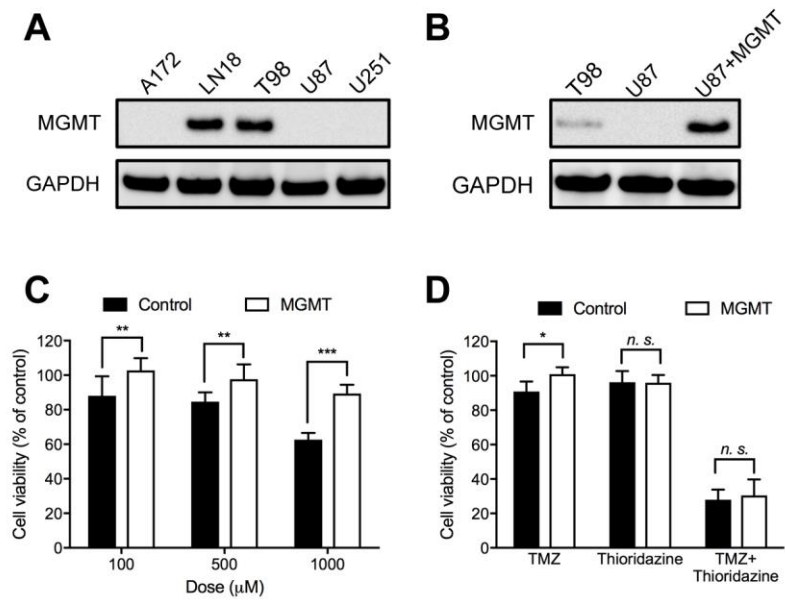


Figure 3

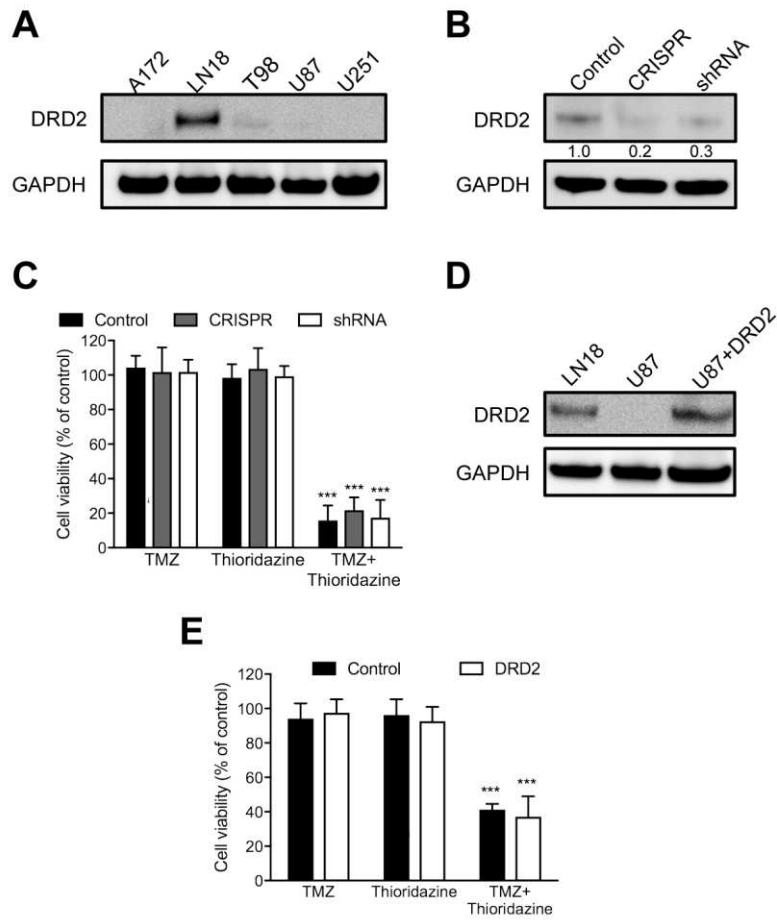


Figure 4

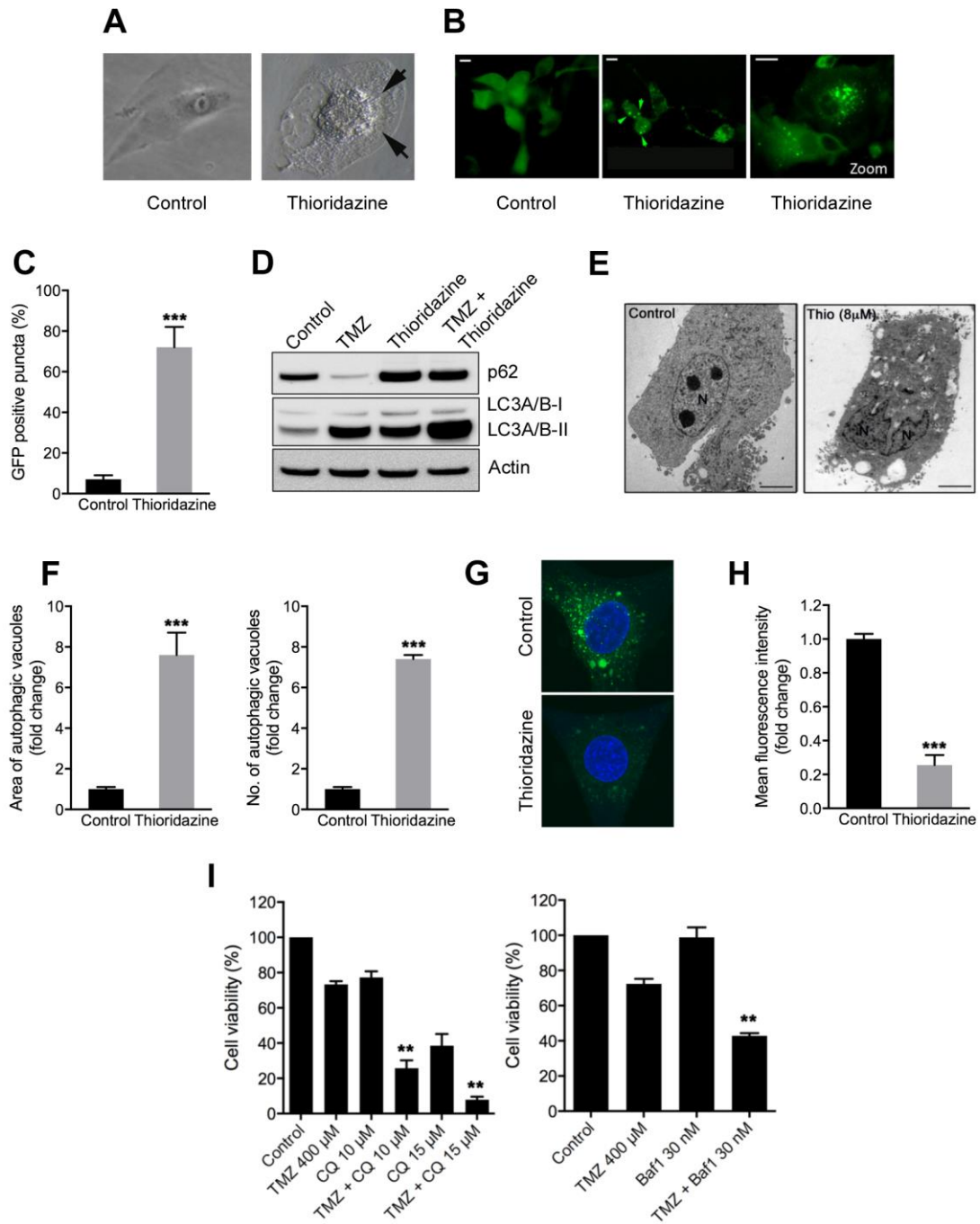


Figure 5

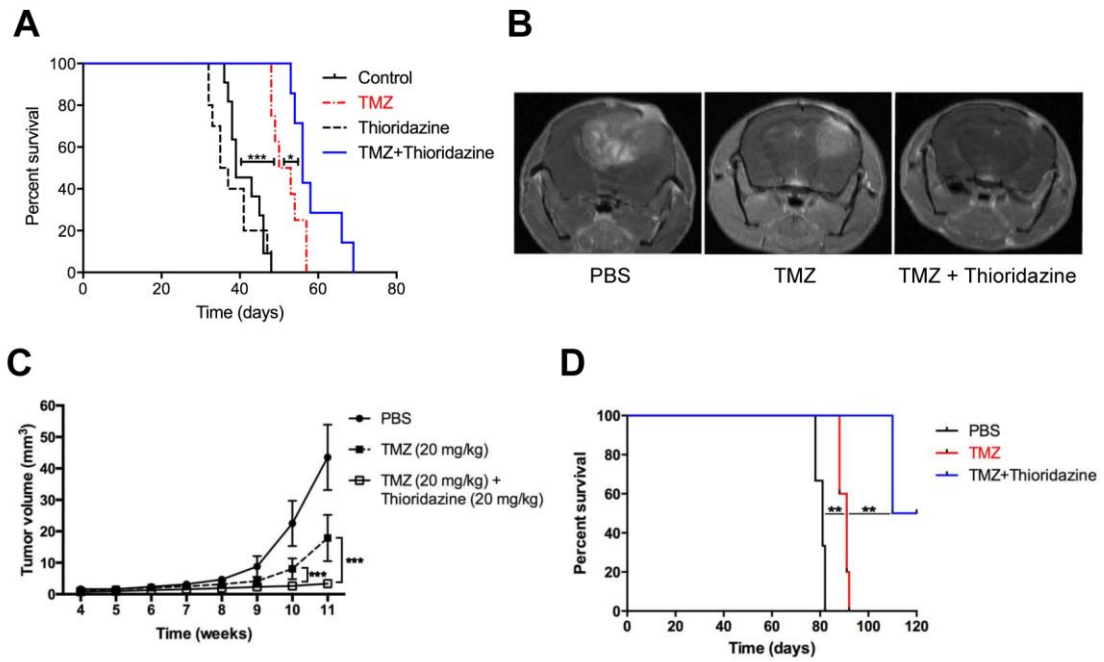
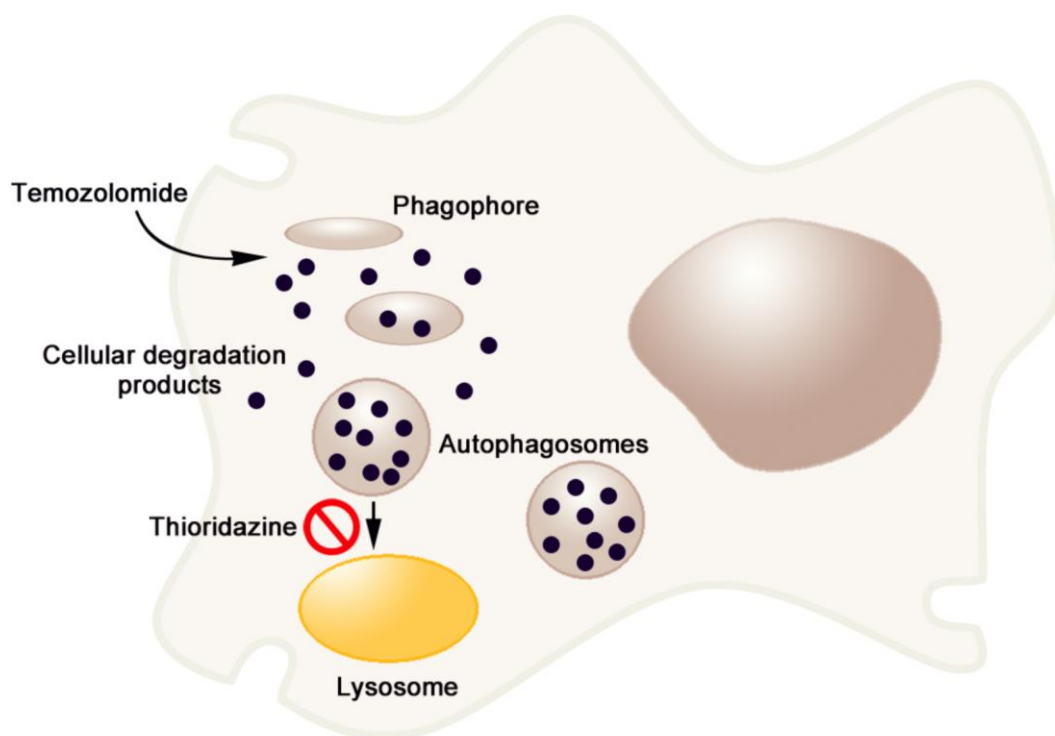


Figure 6



Resistance to Temozolomide (TMZ) is the main cause of treatment failure in patients with Glioblastoma Multiforme (GBM). Although controversial, the ability of TMZ to increase autophagy flux is believed to support cancer growth. The authors identified dopamine antagonist Thioridazine as a potent sensitizer of TMZ cytotoxicity acting through impairment of late-stage autophagy in GBM cells. Thioridazine, combined with TMZ, inhibited tumor growth *in vivo* and increased survival in tumor-bearing animals. This study demonstrates the feasibility of linking results from large-scale genome-wide RNAi studies with corresponding drug-induced alterations in gene expression and underscores the therapeutic relevance of attenuating autophagy in GBM.

# THE DIFFERENCE OF BREAKTHROUGH MOMENTS

WITH AN INTEGRATED SOLUTION FOR  
GROUNDBREAKING SINGLE-CELL RESEARCH

BD Accuri™ C6 Plus Personal Flow Cytometer

BD FACSCelesta™ Cell Analyzer

BD LSRFortessa™ X-20 Cell Analyzer

BD FACSMelody™ Cell Sorter

FlowJo™ Software

One of the largest portfolios of reagents

Discover more >

